CHAPTER III

ASYMMETRIC MONO-OXAZINE: AN INEVITABLE PRODUCT FROM MANNICH REACTION OF BENZOXAZINE DIMERS

Abstract

The Mannich reaction is detailed, which was carried out on benzoxazine dimers under various conditions, that is, temperature, reaction time, and solvents. Against our expectation, in any condition, instead of generating a disubstitution oxazine compound, the reaction gives a product with only a single oxazine ring, a mono-oxazine benzoxazine dimer, as characterized by FT-IR, ^{1}H NMR, ^{13}C NMR, 2D NMR (^{1}H-^{1}H COSY, ^{1}H-^{13}C HMQC, and ^{1}H-^{13}C HMBC), and EA. The asymmetrical reaction is found to be based on the original structure of the benzoxazine dimer which has two phenol rings in a different stability as clarified by X-ray structure analysis of the single crystal. All types of benzoxazine dimers indicate the specific structure with a pair of inter- and intramolecular hydrogen bonds. The bond distance indicates that the intramolecular hydrogen bonding is very strong, while the packing structure emphasizes the high stability of the dimer unit and implies the deactiviation of one phenol ring in the benzoxazine dimer. In this contribution, we demonstrate one of the quite rare examples, showing how the stereostructure of the reactant molecule is an important factor to control the reaction and give an asymmetric product which we never expected when considering only the chemical formula.

Introduction

Polybenzoxazine is known as a polymer with a chemical structure of aza-methylene phenol repeating unit (Scheme 1, eq 1) obtained from the ring-opening polymerization of benzoxazine monomers.[1-5] Benzoxazine monomers, thus, can provide linear or cross-linked polymers, depending on the reaction occurring at ortho and additional para positions. In the cases of some unique monomers, that is, bisphenol-based benzoxazines (Scheme 1, eq 2), Ishida et al. showed a successful polymerization to obtain a series of thermosetting polymers and proposed a novel phenolic resin.[2-3] When it comes to the simple phenol-based benzoxazine monomers, it is interesting to find that few studies have been done. For example, in the case of para-substituted phenol based benzoxazines (Scheme 1, eq 3), it can be expected to obtain linear polymers. However, on the basis of the kinetic studies, Riess et al. found that the polymerization of *p*-cresol proceeded with a limit of four to six repeating units.[5] In addition, this number of repeating units might not be quantitatively exactly determined. Until now, the involved factors and the mechanisms controlling this polymerization have not been clarified.

Recently, to propose a novel supramolecular structured benzoxazine our group focused on the unique structures of polybenzoxazines which resemble those of calixarenes.[6] Here, to achieve our molecules as calixarenes, we came to the point of preparing a well-defined structured benzoxazine, such as a linear or cyclic oligobenzoxazine, based on the ring-opening polymerization of benzoxazine monomers. In such cases, the work can be simplified if we start from the para-substituted phenol in the preparation of benzoxazine monomer followed by the polymerization. However, to our surprise, the para-substituted phenol-based benzoxazine monomers gave us neither the linear oligomer nor the polymer but mainly the dimer in polymerization process even though the reaction conditions were varied.[7] It is important to clarify the reasons why benzoxazine dimers show the self-termination in the polymerization process, which will be reported elsewhere[7]. To achieve our designed molecules as mentioned above, we must overcome the problems of self-termination at the dimer level. In other words, the preparation of linear oligobenzoxazines ($n > 2$) needs other unique strategies to process the reaction to

obtain a linear oligobenzoxazine. Previously, Ishida et al. reported multistep reactions to obtain a linear chain using bromo-substituted phenols.[8] Although the linear benzoxazines were achieved, the reaction was rather complicated, and the final product yield was low while the costs of the synthesis are high.[8] Thus, the method does not seem to be practical to obtain our required product.

Since we can obtain the benzoxazine dimers in a high yield (80-90%),[7] it is one of the approaches to apply these dimers as a starting material. We propose alternative steps of an oxazine cyclization and a ring-opening reaction of benzoxazine dimers to obtain a well-defined cyclic compound. As will be described in the present work, to our surprise again, a Mannich reaction of benzoxazine dimer does not proceed to give dioxazine compounds as expected in Scheme 2 (compound **4**), but gives an asymetric product with the single oxazine ring at an alternative phenol (Scheme 2, compound **5**). Even when the reaction conditions are varied, we obtain only an asymmetric mono-oxazine dimer as a product. At this point, without clarification of the reaction of dimers and the key factors involved, we cannot continue our strategies to obtain a well-defined benzoxazine structure. We have to clarify the reason the imbalance-structured compound is obtained inevitably. In another words, it is important to note that this asymmetric mono-oxazine product is always produced without any specific condition or catalyst.

Thus, in the present contribution, we (i) maintain that our basic studies on the Mannich reaction of benzoxazine dimer clarifying the structure of the compound obtained based on various aspects of analyses, especially the 2D-NMR, (ii) identify the factor that originates the asymmetric reaction, and (iii) show how the factor studied can be applied in the mechanism to explain the inevitable generation of mono-oxazine compounds. The clarification of the specific reaction occurring in benzoxazine dimers will be a useful guideline for a reasonable molecular design to obtain a well-defined supramolecular benzoxazine in the future.

Results and Discussion

Mannich Reaction of the Benzoxazine Dimer. Compound **1** (Scheme 3) was used as a model dimer to react with formaldehyde and cyclohexylamine via the Mannich reaction. From FT-IR data, the compound obtained gives rise to a broad band at 3000-2800 cm^{-1}, similar to **1**, implying the existence of strong hydrogen bonds. In fact, Daimay et al.[9] reported that the cyanuric acid shows an infrared band corresponding to the strong OH---N hydrogen bonding in the frequency region of 3200-2600 cm^{-1}. The band at 3215 cm^{-1} due to the intermolecular hydrogen bond is observed for compound **1** but cannot be observed in the compound obtained. The bands at 1514 and 1500 cm^{-1} which are intrinsic to the dimer, were changed to a singlet at 1498 cm^{-1} which is attributed to the vibration mode of the oxazine.

From the Mannich reaction, the structure of the product obtained from **1** can be proposed as either **4** or **5** (Scheme 2). It should be noted that compound **4** consists of three different methylene groups and three cyclohexyl groups, while compound **5** consists of four different methylene groups and two different cyclohexyl groups. ^{1}H NMR spectra of the product obtained from **1** show four types of methylene groups at δ_H = 3.57, 3.78, 4.03, and 4.98 ppm as singlet resonances, while the corresponding ^{13}C NMR spectra show carbon resonance at δ_C 47.38, 47.87, 52.89, and 80.19 ppm. These data suggest the preferability of **5** for the compound in question. Four different methylene groups correlate to two sets at 4.03 and 4.98 ppm and at 3.57 and 3.78 ppm, suggesting the existence of the methylene groups of the aza linkage and of the oxazine ring (Table 1).

In another step, the structure of **5** can be identified by confirming cyclohexyl protons presented in the structure. The number and the position of the cyclohexyl groups on each nitrogen atom were studied by the ^{1}H-^{1}H COSY. Figure 1 shows the two cyclohexyl groups appearing in different position. The cyclohexyl groups can be distinguished clearly into two groups by resonances of methine protons of H7 and H11. However, the protons remaining (H8 to H10, H8' and H9', H12 to H14, H12' and H13') cannot be identified for the exact position in the structure because of the possibility of being vicinal and geminal protons, including axial and equatorial protons

in the cyclohexyl structure. In addition, ^{1}H-^{13}C HMBC (Figure 2) shows the interaction between methylene protons, that is, between H5, H6, and C7 of cyclohexyl group, and that between H3 and C11, implying the asymmetric structure of compound **5**.

On the assumption of an asymmetric structure such as **5**, the protons of each aromatic ring can be distinguished into two and three species, which should be observed from the correlation shift and the different coupling constants (*J*). As shown in Table 1, the values of *J* for H17, H19, H23, H25, and H26 indicate the different species of protons. This supports the asymmetric structure of **5**. Here, the two equivalent aromatic protons (C17 and C19) are difficult to distinguish. The interaction between methylene groups with aromatic carbons in the HMBC mode helps us clarify. As shown in Table 1 and Figure 3, the methylene protons, H6, show the interaction only with aromatic carbon of C17, while aromatic protons, H17 and H19, interact with aromatic carbon C6 (Table 1). Another set of methylene protons H3 interacts with the aromatic carbon C23, while a set of aromatic protons H23 interacts with C3 of methylene group. This suggests that there is one oxazine ring unit linked by an aza-methylene bridge to the phenyl ring, as shown in structure **5**.

The phenol ring is also confirmed from the presence of the hydroxyl resonance at 11.16 ppm. In addition, the methyl group of the phenol ring appears in the ^{13}C NMR spectrum at 20.47 ppm, while the other of the benzoxazine ring is found at 20.59 ppm. Methyl protons H1 interact with aromatic carbons, C22, C23, C24, and C26, while other methyl protons H2 interact with aromatic carbons, C17 and C19. In this way, all of the data of the NMR spectra support the chemical formula of **5** in Scheme 3 as the compound obtained from the Mannich reaction of **1**.

Another important experimental result to support this conclusion is the data of EA. On the assumption of the dioxazine unit, the EA should give %C 77.95, %H 9.40, and %N 7.18, respectively. However, the analyzed result gives %C 77.79, %H 9.17, and %N 6.09, which are quite close to the calculated data for the dimer with a single oxazine unit: %C 77.92, %H 9.10, and %N 6.06. This excellent agreement indicates also that dimer **1** yields only compound **5** and does not give any product such as compound **4**.

Solvent Polarity Effect. In each reaction, dimer **1**, **2**, or **3**, was found to dissolve well in dioxane, resulting in an homogeneous system for benzoxazine preparation. After 6 h at the reflux temperature of dioxane, the reaction was completed to give mono-oxazine with the yield of 75-80%. In contrast to the case of dioxane, the dimer was rather difficult to dissolve in cyclohexane. The reaction started as an heterogeneous system but turned into an homogeneous after the completion of the reaction. The yield obtained in cyclohexane was the same as that obtained from dioxane.

A polar solvent such as methanol was also used. The system gave low yields (20-30%), and the product was a yellowish viscous solution. This implies that the high polarity of the solvent affects the mono-oxazine formation. After recrystallization, the product was identified to be the mono-oxazine one.

To exclude the solvent effect, we attempted the reaction in a neat liquid state. The dimer **1** was heated to a temperature higher than the melting point (135 °C), and formaldehyde and cyclohexylamine were added. The reaction was completed within 15 min. After recrystallization, the yield of the product **5** was found to be 75-80%.

In all the cases, the compounds obtained were mono-oxazine derivatives as characterized by FT-IR and NMR. It should be noted that the mono-oxazine benzoxazine dimer was formed in a high yield even at the diversified reaction conditions, that is, polarity (dioxane, cyclohexane, methanol) and temperature (60 °C for methanol, 80 °C for cyclohexane, 100 °C for dioxane, and 135 °C for molten state systems). This indicates that the mono-oxazine benzoxazine dimer is a stable compound and the reaction is terminated almost always at the stage of the formation of only one oxazine unit, against our earlier prediction.

Molar Ratio of Reactants. It is important to clarify whether the mono-oxazine benzoxazine dimer comes from incomplete reaction or is a product of the inevitable pathway. Judging from the equation of chemical reaction shown in Scheme 2, the production of the compound **5** might be a result of incomplete reaction. The ratio of formaldehyde and amine was increased further to get the dioxazine product.

However, even when the ratio was increased to 1:8:4, the compound **5** was obtained in a similar yield. In contrast, the decrement of the ratio to half, that is, dimer:formaldehyde:amine = 1:2:1 also gave the compound **5** with the yield of 75-85%. In this way, only the mono-oxazine product was obtained irrespective of the molar ratio of reactants. In other words, the benzoxazine with a single oxazine unit is a reaction product of the "inevitable pathway".

It is also necessary to show that not only dimer **1** but also other benzoxazine dimers give mono-oxazine derivatives. Here, we studied the Mannich reaction on dimers **2** and **3**. The structural studies by FT-IR, NMR, and EA indicate that **2** and **3** give the mono-oxazine compounds of **6** and **7**, respectively.

Crystal Structure and the Stability of Benzoxazine Dimer. We speculated that the asymmetric product might come from the different circumstances of the two phenol groups in a molecule which induced the different activity. For example, Dunkers et al.[10] and Schnell et al.[11] applied *N*,*N*-bis(3,5-dimethyl-2-hydroxybenzyl) methylamine as a benzoxazine model compound to study the conformation of polybenzoxazine resins and reported the existence of inter- and intramolecular hydrogen bondings between the nitrogen atom of the aza group and the hydroxy group of phenol by using FT-IR data and the X-ray structure analysis. However, the detailed information concerning the bond length and bond angle of the intramolecular hydrogen bond was not clarified at all. Moreover, they did not notice at all an intimate relationship of this intramolecular hydrogen bonding with the reaction of the dimer. As will be mentioned below, we speculated the possibility that the asymmetric reaction might originate from the imbalance reactivity of the phenol group; one phenol group is constrained by an intramolecular hydrogen bond while the other phenol is not.

The X-ray structural analyses of dimers were successfully done for the compounds **1**, **2**, and **3**. The difference synthesis F_o-F_c gave definitely the position of the hydrogen atom participating in the intramolecular hydrogen bond. Figure 4 shows an example of **1** having a strong intramolecular hydrogen bond between the aza group and the phenol with the distance of O-H---N 1.80 Å, O---N 2.62 Å and O-H---O 2.41

Å. The intermolecular hydrogen bonding is formed between the two adjacent dimers with the distance of O-H---O 1.77 Å and O---O 3.04 Å. In this way, for all of the dimers investigated here, the strong inter- and intramolecular hydrogen bonds are observed. Table 2 summarizes some of the molecular parameters revealed for compound **1**. Crystallographic data including fractional coordinates of atoms are given in Table 3. The structural analyses for the other compounds will be reported elsewhere.[12]

As mentioned above, the two phenol groups are subjected to quite different circumstances. Although this observation can be made for the solid-state samples, a similar situation may be expected to occur even in the solution where our reaction was proceeded. In fact, Dunker et al.[10] reported the existence of intramolecular hydrogen bonding in the solution of chloroform. The intramolecular hydrogen bonding can be maintained even in the molten state, as reported by Dunker et al.[10] for bisphenol A-based benzoxazine. In this way, the intramolecular hydrogen bonds can be formed stably in the various states of the benzoxazine molecule. Thus, we propose here that the reactive sites of the dimer rae reduced to one by stabilization through an intramolecular hydrogen bond. In other words, one of the phenol rings becomes inactive owing to the intramolecular hydrogen bond of O-H---N, giving an asymmetrically structured product. This can be seen for most of the dimers investigated thus far.

Speculated Mechanism. The mechanism proposed by Burke et al.[13] can be applied to explain the reaction. Owing to the intramolecular hydrogen bonding, a single phenol group in the dimer is stabilized. As a result, the oxazine formation can be achieved only at the other phenol group where the intermolecular hydrogen bond is formed. When one of the phenol rings is deactivated in this way by the intramolecular hydrogen bond, the electrophilic substitution of the iminium ion will occur only on the alternate phenol ring at its ortho position. The cyclization to form the oxazine ring then occurs after the loss of a water molecule.

Experimental Section

Chemicals. Paraformaldehyde was purchased from Sigma (U.S.A.). 4-Ethylphenol, *p*-cresol, cyclohexylamine, and propylamine were obtained from Fluka Chemicals (Buchs, Switzerland). 1,4-Dioxane, methanol, cyclohexane, sodium hydroxide, sodium sulfate anhydrous, and diethyl ether were products from Ajax chemicals (Australia). All chemicals were AR grade and used without further purification.

Instruments. Fourier transform infrared spectra were measured at a resolution of 4 cm^{-1} by using a Bruker Equinox55/S spectrophotometer equipped with deuterated triglycine (DTGS) detector under the constant purge with dry air. The ^{1}H- and ^{13}C nuclear magnetic resonance (NMR) spectrometers were a Varian UNITYplus 600 with proton frequency of 600 MHz. The coaddition of 64 transients for ^{1}H NMR spectra and 960 transients for ^{13}C NMR spectra gave sufficient signal-to-noise ratio. The repeating time for ^{1}H experiments was 6 s for obtaining the proper integration value. The repeating time for ^{13}C experiments was 3 s. ^{1}H-^{1}H Correlated Spectroscopy (COSY), ^{1}H-^{13}C Heteronuclear Multiple Quantum Coherence (HMQC) and ^{1}H-^{13}C Heteronuclear Multiple-Bond Coherence (HMBC) were performed. The samples were prepared as solutions using deuterated chloroform solvent with tetramethylsilane (0.1%, w/w) as an internal reference. Elemental analysis (EA) was performed by using a Perkin-Elmer 2400 Series II CHNS/O analyzer with the combustion temperature of 975 °C and a reduction temperature of 500 °C. For single crystals of benzoxazine dimers, that is, compounds **1**, **2**, and **3**, an X-ray imaging plate system DIP3000 (MAC Science Co. Ltd., Japan) was used. The graphite-monochromatized Mo Kα line (λ = 0.71073 Å), which was generated from the SRA-M18XHF rotating anode X-ray generator (50 kV and 200 mA), was used as an incident X-ray source. The data collection was performed by the XDIP software (MAC Science). The sample was oscillated in a range of 3° over a total rotation angle of 0-180° around the ω axis. The exposure time was 30 min for one image. It took about 12 h to collect the 24 images in total. The data were analyzed by using

the software DENZO and SCALEPACK.[14-15] The crystal structure was solved by using a software maXus (NoniusBV, Delft). The direct method was used to find out the initial models, where the software SIR92 developed by Altmare et al. was used.[16] Least-squares refinement was made on the basis of the full matrix method by using the quantity $\Sigma\omega(|F_o|^2-|F_c|^2)^2$ as a minimized function with the weight $\omega = exp[FA \sin^2\theta/\lambda^2]/[\sigma^2(F_o)+FBF_o^2]$, where $\sigma^2(F_o)$ was the squared standard deviation of the observed structure factor F_o and the coefficients FA and FB were set to the values 0.0 and 0.03, respectively. The reflections satisfying the cutoff condition of $|F_o| > 3\sigma(|F_o|)$ were used in the least-squares refinement. Because no detectable effect was found, the absorption correction for the observed intensity was not included in the structural refinement. As the measure of the reasonableness of the structural analysis, the reliability factors, R and R_w, were defined by the following equations; $R = \Sigma||F_o|-|F_c||/\Sigma|F_o|$ and $Rw = [\Sigma\omega(|F_o|-|F_c|)^2/\omega|F_o|^2]^{1/2}$.

Syntheses. Symmetric benzoxazine dimers (Scheme 3), *N*,*N*-bis(2-hydroxy-5-methylbenzyl)cyclohexylamine **1**, *N*,*N*-bis(2-hydroxy-5-ethylbenzyl)cyclo hexylamine **2**, and *N*,*N*-bis(2-hydroxy-5-methylbenzyl)propylamine **3**, were prepared as reported elsewhere[7] and used as starting materials.

Preparation of 3,4-dihydro-3-cyclohexyl-6-methyl-8-((2'-hydroxy-5'-methyl benzyl)cyclohexylaminomethyl)-2H-1,3-benzoxazine, 5. Cyclohexylamine (1.15 mL, 10 mmol) was added dropwise into the solution of paraformaldehyde (0.63 g, 20 mmol) in dioxane (10 mL). Benzoxazine dimer **1** (1.70 g, 5 mmol) in 20 mL of dioxane was further added and the solution was refluxed for 6 h. The dioxane was removed in vacuo to obtain a yellowish viscous product. The solution obtained was dissolved in 50 mL of diethyl ether and extracted with 3 N NaOH 10 mL for three times, followed by 10 mL of water washing until the solution became neutral. The product was dried over sodium sulfate, and the solvent was removed. The crude viscous product was left overnight at room temperature, producing a white precipitate. The precipitate was collected and recrystallized by 2-propanol.

To study the solvent effect, the similar reactions were carried out using cyclohexane and methanol as solvents. The reaction in a neat liquid state at 135 °C for 15 min was also performed for comparison. The molar ratios of reactants were also varied, that is, paraformaldehyde (0.32 g, 10 mmol), cyclohexylamine (0.56 mL, 5 mmol) and benzoxazine dimer **1** (1.70 g, 5 mmol).

Compound **5**: 80% yield; R_f = 0.29 (5% MeOH in $CHCl_3$); mp = 130 °C; FT-IR (KBr, cm^{-1}): 3300-3100 (br, OH), 1498 (s, oxazine), 1223 (br s, C-O); ^{1}H NMR (600 MHz, $CDCl_3$, ppm): δ_H 1.12 (2H, m, CH_2), 1.16 (2H, m, CH_2), 1.25 and 1.98 (4H, m, CH_2), 1.40 and 1.92 (4H, m, CH_2), 1.58 and 1.74 (4H, m, CH_2), 1.60 and 1.76 (4H, m, CH_2), 2.21 (3H, s, Ar-CH_3), 2.20 (3H, s, Ar-CH_3), 2.62 (1H, tt, CH, J_1 = 11.81 Hz and J_2 = 3.30 Hz), 2.68 (1H, m, CH), 3.57 (2H, s, Ar-CH_2-N), 3.78 (2H, s, Ar-CH_2-N), 4.03 (2H, s, Ar-CH_2-N), 4.98 (2H, s, O-CH_2-N), 6.64 (1H, d, Ar-H, J_3 = 8.24 Hz), 6.66 (1H, d, Ar-H, J_4 = 1.51 Hz), 6.74 (1H, d, Ar-H, J_5 = 1.94 Hz), 6.83 (1H, d, Ar-H, J_4 = 1.51 Hz), 6.89 (1H, dd, Ar-H, J_3 = 8.24 Hz and J_5 = 1.94 Hz), 11.16 (1H, br, Ar-OH); ^{13}C NMR (150 MHz, $CDCl_3$, ppm): δ_C 20.47, 20.55, 25.48, 25.94, 26.01, 26.30, 27.64, 31.60, 47.38, 47.87, 52.89, 57.99, 58.47, 80.19, 115.63, 121.19, 122.45, 124.91, 126.76, 127.48, 128.52, 128.71, 129.04, 130.18, 151.58, 155.94. Anal.calcd for $C_{30}H_{42}N_2O_2$: C, 77.92; H, 9.10; and N, 6.06. Found: C, 77.79; H, 9.17; and N, 6.09.

Preparation of 3,4-dihydro-3-cyclohexyl-6-ethyl-8-((2'-hydroxy-5'-methyl benzyl)cyclohexylaminomethyl)-2H-1,3-benzoxazine, 6 and 3,4-dihydro-3-cyclohexyl-6-methyl-8-((2'-hydroxy-5'-methylbenzyl)propylaminomethyl)-2H-1,3-benzoxazine, 7. Benzoxazine dimer **2** (1.84 g, 5 mmol), paraformaldehyde (0.32 g, 10 mmol), and cyclohexylamine (0.56 mL, 5 mmol) were used to prepare compound **6**, while benzoxazine dimer **3** (1.50 g, 5 mmol), paraformaldehyde (0.32 g, 10 mmol), and propylamine (0.42 mL, 5 mmol) were used to prepare compound **7**. Similarly, the reactions proceeded in a neat liquid state at 135 °C for 15 min. The obtained products were characterized using FT-IR, ^{1}H NMR, ^{13}C NMR, and EA.

Compound **6**: 80% yield; R_f = 0.27 (5% MeOH in $CHCl_3$); mp =143 °C; FT-IR (KBr, cm^{-1}): 3300-3100 (br, OH), 1498 (s, oxazine), 1198 (br s, C-O). ^1H NMR (600 MHz, $CDCl_3$, ppm): δ_H 1.08 (2H, m, CH_2), 1.15 (2H, m, CH_2), 1.19 (6H, t, CH_3-CH_2-Ar, J_1 = 7.69 Hz), 1.25 and 1.98 (4H, m, CH_2), 1.40 and 1.91 (4H, m, CH_2), 1.58 and 1.75 (4H, m, CH_2), 1.60 and 1.79 (4H, m, CH_2), 2.52 (4H, q, CH_3-CH_2-Ar, J_1 = 7.69 Hz), 2.63 (1H, tt, CH, J_2 = 11.97 Hz and J_3 = 3.42 Hz), 2.71 (1H, m, CH), 3.59 (2H, s, Ar-CH_2-N), 3.81 (2H, s, Ar-CH_2-N), 4.05 (2H, s, Ar-CH_2-N), 4.99 (2H, s, O-CH_2-N), 6.67 (1H, d, Ar-H, J_4 = 8.12 Hz), 6.68 (1H, d, Ar-H, J_5 = 2.14 Hz), 6.77 (1H, d, Ar-H, J_6 = 1.71 Hz), 6.86 (1H, d, Ar-H, J_5 = 2.14 Hz), 6.93 (1H, dd, Ar-H, J_4 = 8.12 Hz, J_6 = 1.71 Hz), 11.22 (1H, br, Ar-OH); ^{13}C NMR (150 MHz, $CDCl_3$, ppm): δ_C 15.67, 15.92, 25.47, 25.94, 26.02, 26.31, 27.68, 27.99, 28.02, 31.59, 47.48, 47.96, 52.95, 58.05, 58.39, 80.15, 115.65, 121.16, 122.43, 124.93, 125.49, 127.30, 127.82, 128.98, 134.14, 135.24, 151.73, 156.16. Anal.calcd for $C_{32}H_{46}N_2O_2$: C, 78.36; H, 9.39; and N, 5.71. Found: C, 78.19; H, 9.44; and N, 5.73.

Compound **7**: 75% yield; R_f = 0.31 (5% MeOH in $CHCl_3$); mp =125 °C; FT-IR (KBr, cm^{-1}): 3350-3100 (br, OH), 1498 (s, oxazine), 1228 (br s, C-O); ^1H NMR (600 MHz, $CDCl_3$, ppm): δ_H 0.83 (3H, t, N-CH_2-CH_2-CH_3, J_1 = 7.33 Hz), 1.13 (2H, m, CH_2), 1.24 and 1.97 (4H, m, CH_2), 1.61 and 1.74 (4H, m, CH_2), 1.65 (2H, qt, N-CH_2-CH_2-CH_3, J_1 = 7.33 Hz and J_2 = 2.06 Hz), 2.21 (3H, s, CH_2), 2.22 (3H, s, Ar-CH_3), 2.42 (2H, t, N-CH_2-CH_2-CH_3, J_2 = 2.06 Hz), 2.68 (1H, m, CH), 3.57 (2H, s, Ar-CH_2-N), 3.68 (2H, s, Ar-CH_2-N), 4.04 (2H, s, Ar-CH_2-N), 4.98 (2H, s, O-CH_2-N), 6.66 (1H, d, Ar-H, J_3 = 8.01 Hz), 6.68 (1H, d, Ar-H, J_4 = 1.49 Hz), 6.74 (1H, d, Ar-H, J_5 = 1.60 Hz), 6.83 (1H, d, Ar-H, J_4 = 1.49 Hz), 6.92 (1H, dd, Ar-H, J_3 = 8.01 Hz and J_5 = 1.60 Hz), 10.83 (1H, br, Ar-OH); ^{13}C NMR (150 MHz, $CDCl_3$, ppm): δ_C 11.83, 19.33, 20.55, 20.66, 25.56, 26.02, 31.65, 47.55, 52.46, 55.32, 57.59, 58.59, 80.30, 115.75, 121.40, 122.48, 124.16, 127.01, 127.72, 128.72, 128.79, 129.16, 130.22, 151.69, 155.89. Anal.calcd for $C_{27}H_{38}N_2O_2$: C, 76.78; H, 9.00; and N, 6.64. Found: C, 76.83; H, 9.07; and N, 6.57.

Conclusions

Although we expected the dioxazine compound as a product from the Mannich reaction onto benzoxazine dimer, we got only mono-oxazine as characterized by FT-IR, ^{1}H NMR, ^{13}C NMR, and 2D-NMR. X-ray structure analysis revealed the existence of intramolecular hydrogen bondings with a distance of ca. 1.8 Å. Here, we want to propose the reaction mode of our benzoxazine dimer as a "self-selective reaction" since the reaction occurs at only the single site of phenol, owing to the intramolecular hydrogen bond of the dimer itself. In other words, the mono-oxazine is produced *inevitably* because of this "self-selective reaction" under the various conditions.

In this way, judging from the chemical formula, it is unexpected to achieve the asymmetric molecule. However, as we clarified here, another key factor is involved in the reaction, that is, the unique stereo structure of the reactant molecule by intramolecular hydrogen bonding has to be taken into consideration. We ought to note that the present work gives us a hint to achieve the asymmetrical product by designing the molecule with a strong intramolecular hydrogen bond to deactivate the reactive site. Hence, with this approach we may obtain the desired product in a high yield without multisteps of protecting and deprotecting procedures, and the use of catalyst, and special condition. We are achieving a series of well-defined polybenzoxazines by making mono-oxazine benzoxazine dimer compounds be a useful pathway.

Acknowledgements. We thank Professor Mikiji Miyata (Department of Material and Life Science, Faculty of Engineering, Osaka University, Japan) and Dr. Keonil Lee (Graduate School of Science, Osaka University, Japan) for NMR measurements. A deep gratitude is expressed to Mr. Seishi Saragai and Mr. Hisakatsu Hama (Department of Macromolecular Science, Graduate School of Science, Osaka University, Japan) for the help in single-crystal analyses. S.C. gratefully acknowledges the financial support of the Hitachi Scholarship Foundation and Japan Society for the Promotion of Science (JSPS). Appreciation is also extended to Dr. Sathorn Suwan (The Center Laboratory Instrument of Chulalongkorn

University, Thailand) for the fruitful discussions on ^{13}C-NMR and 2D-NMR interpretation.

References

1. Burke, W. J.; Bishop, J. L.; Mortenson, E. L.; Bauer, W. N. *J. Org. Chem.* **1965**, *30*, 3423.
2. Ning, X.; Ishida, H. *J. Polym. Sci., Part A: Polym. Chem.* **1994**, *32*, 921.
3. Ning, X.; Ishida, H. *J. Polym. Sci., Part A: Polym. Chem.* **1994**, *32*, 1121.
4. Dunkers, J.; Ishida, H. *Spectrochimi. Acta* **1995**, *51A*, 855.
5. Riess, G.; Schwob, J. M.; Guth, G.; Roche, M.; and Laude, B., *Advances in Polymer Synthesis, Polymer Science and Technology*; Culbertson, B. M.; McGrath, J. E., Eds.; Plenum: New York; 1985; Vol. 31, pp 27-49.
6. Chirachanchai, S.; Laobuthee, A.; Phontamrag, S.; Siripattanasarakit, W.; Ishida, H. *J. Appl. Polym. Sci.* **2000**, *77*, 2561-2568.
7. Laobuthee, A.; Chirachanchai, S.; and Ishida, H., In preparation.
8. Ishida, H.; Krus, C. M. *Macromolecules* **1998**, *31*, 2409.
9. Lin-Vien, D.; Colthup, N. B.; Fateley, G. W.; and Grassel, G. J. *Infrared and Raman Characteristic Frequencies of Organic Molecules*; Academic Press: 1991; pp 296.
10. Dunker, J.; Zarate, E. A.; Ishida, H. *J. Phys. Chem.* **1996**, *32*, 13514-13520.
11. Schnell, I.; Brown, S. P.; Low, H. Y.; Ishida, H.; Spiess, H. W. *J. Am. Chem. Soc.* **1998**, *120*, 11784.
12. Chirachanchai, S.; Laobuthee, A.; and Tashiro, K., In preparation.
13. Burke, W. J. *J. Am. Chem. Soc.* **1949**, *71*, 609.
14. Otowinowski, Z.; Minor, W. *Methods Enzymol.* **1997**, 276.
15. Otowinowski, Z.; Minor, W. *Macromolecular Crystallography: Part A*; Carter Jr., C. W.; Sweet, R. M., Eds.; Academic Press: London, 1997; pp 307.
16. Altmare, A.; Cascarano, G.; Giacovazzo, C.; Guagliardi, A.; Burla, M. C.; Polidori, G.; Camalli, M. *J. Appl. Crystallogr.* **1994**, *27*, 435.

Figure Captions

Figure 1. ^{1}H-^{1}H COSY correlation spectra of mono-oxazine benzoxazine dimer **5**.

Figure 2. ^{1}H-^{13}C HMBC correlation spectra of mono-oxazine benzoxazine dimer **5**.

Figure 3. ^{1}H-^{13}C HMBC correlation spectra of mono-oxazine benzoxazine dimer **5**.

Figure 4. Dimer **1** packing structure.

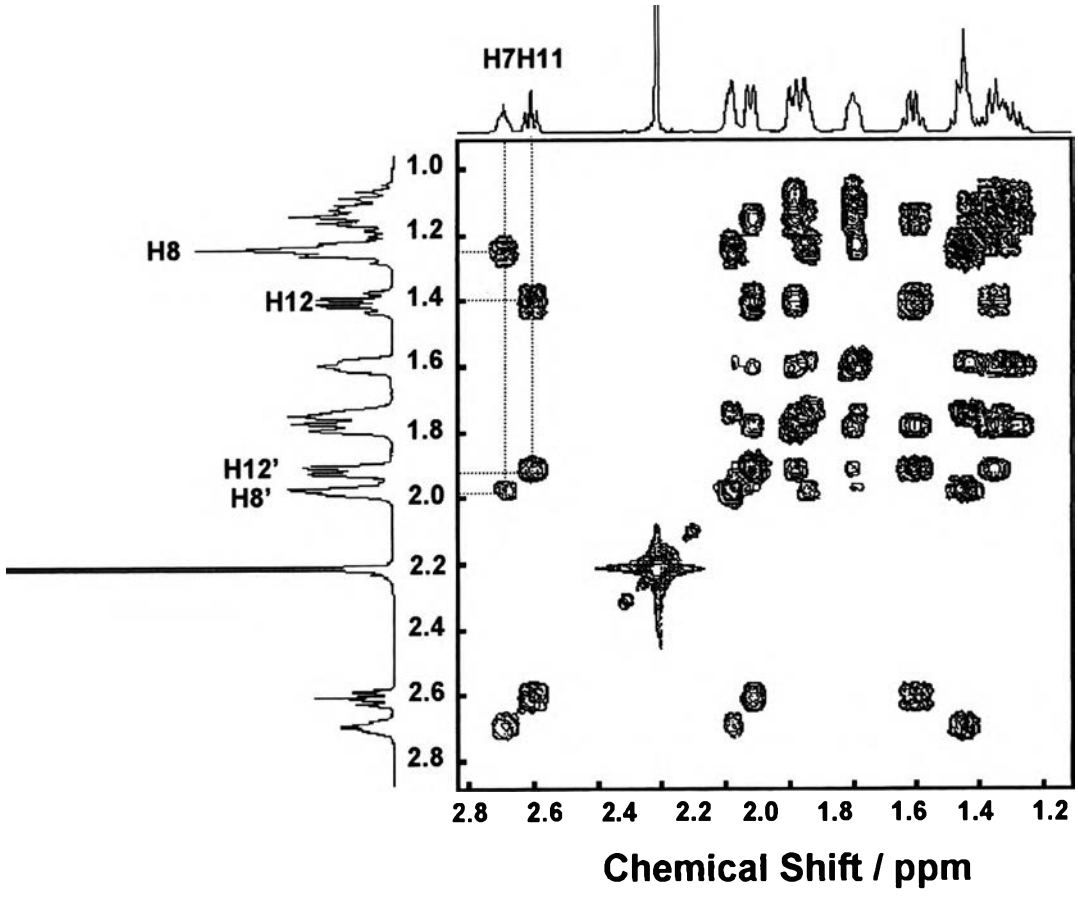

Figure 1. (Apirat et al.)

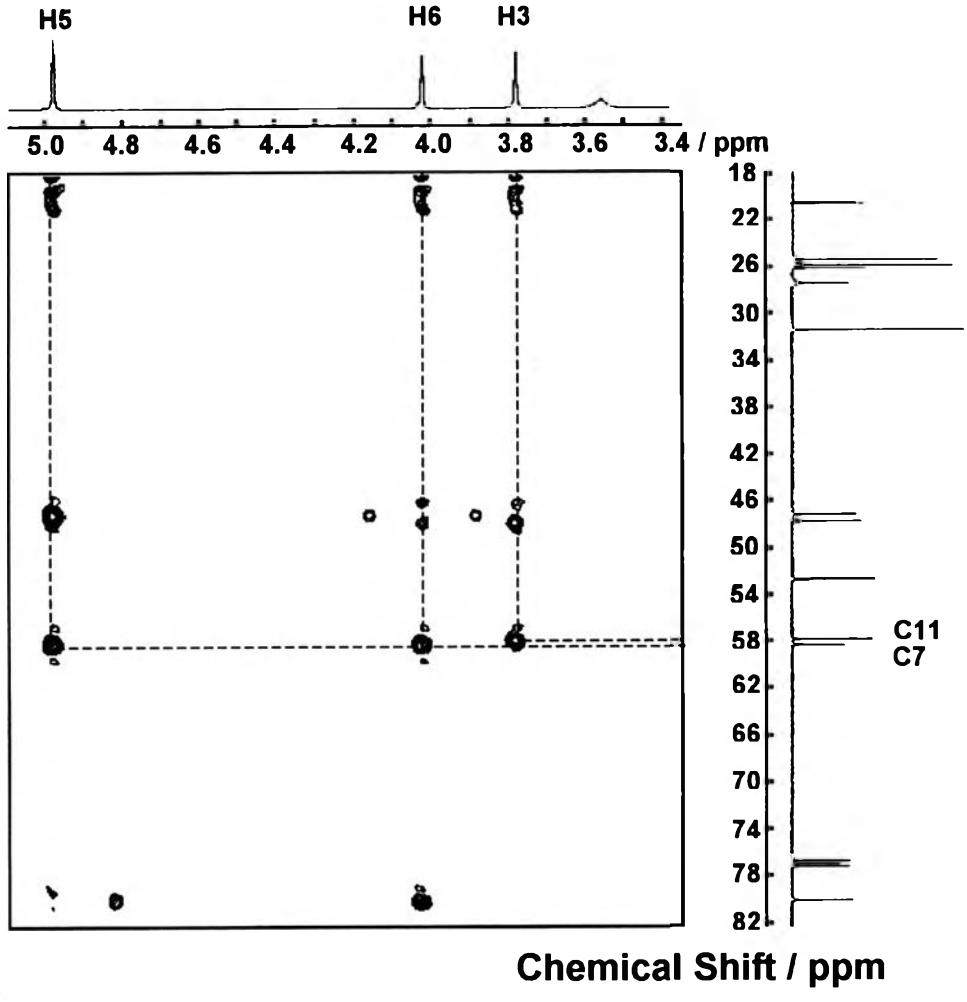

Figure 2. (Apirat et al.)

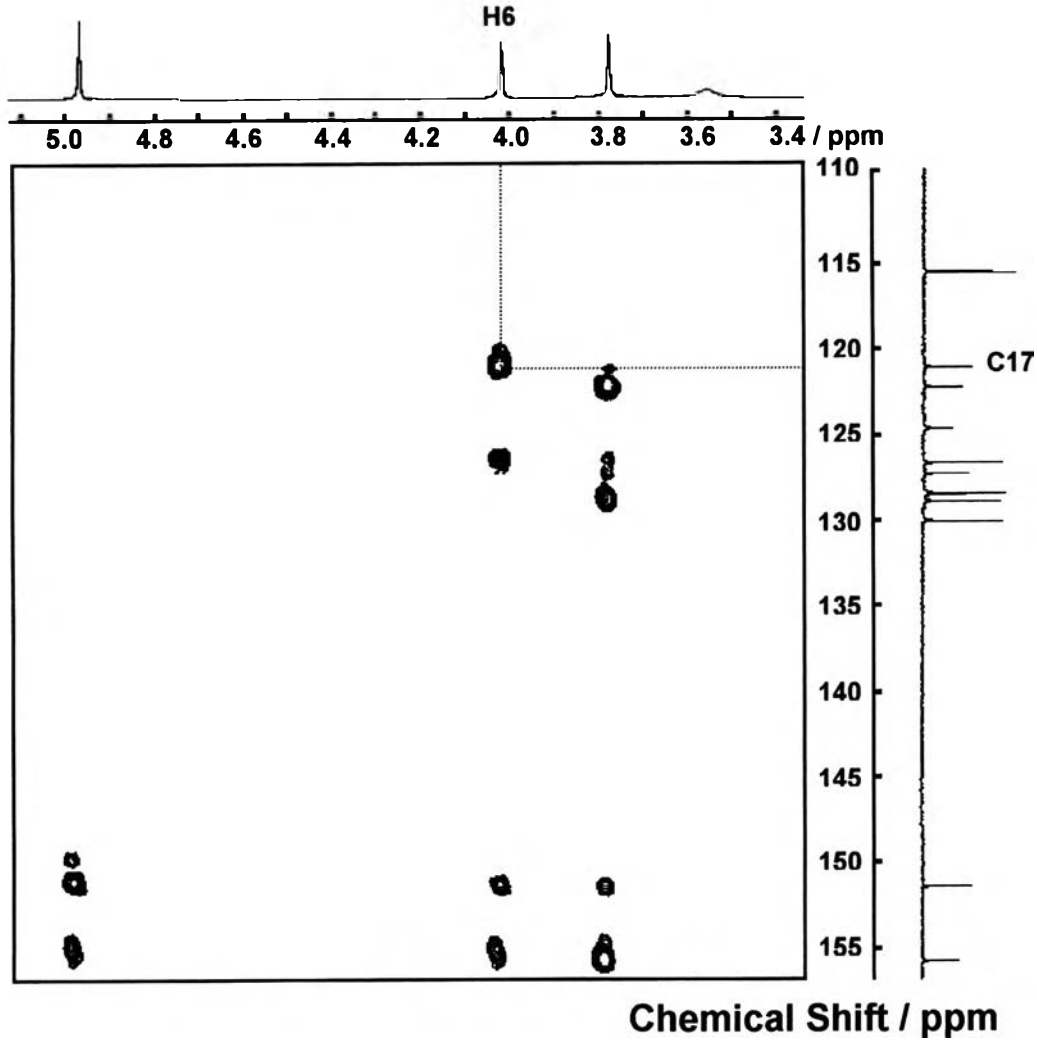

Figure 3. (Apirat et al.)

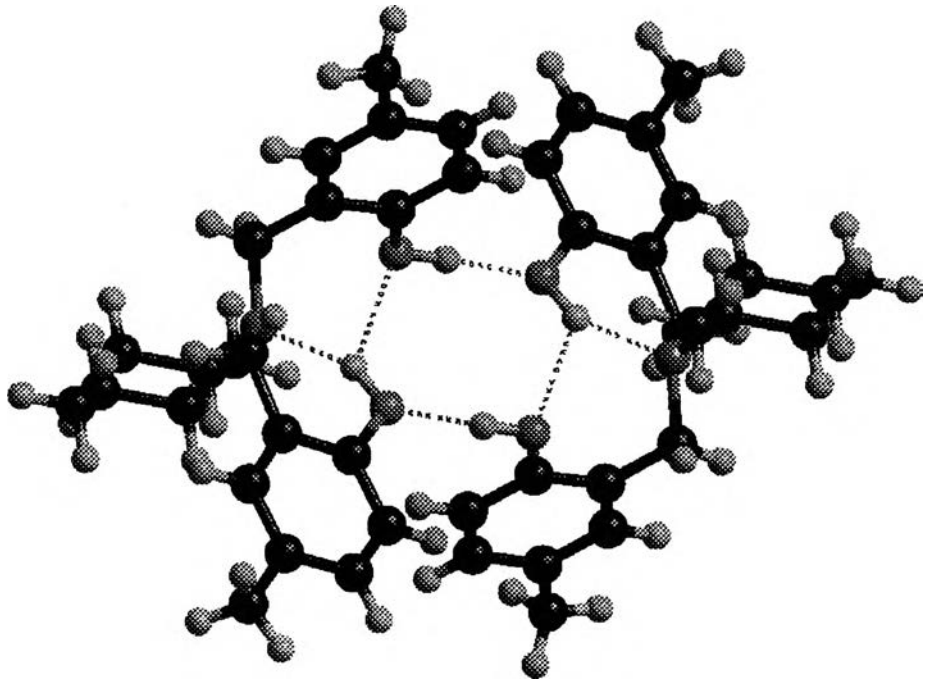

Figure 4. (Apirat et al.)

Table Captions

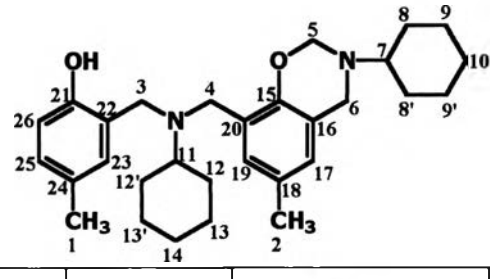

Position	^{1}H δ_H, multi. [*J* (Hz)]	^{13}C δ_C	^{1}H-^{1}H COSY	^{1}H-^{13}C HMBC
1	2.21, 3H, s	20.47	H26, H23	C23, C24, C26
2	2.20, 3H, s	20.59	H17, H19	C17, C18, C19
3	3.78, 2H, s	52.89	-	C1, C4, C11, C15, C21, C22, C23
4	3.57, 2H, s	47.87	-	-
5	4.98, 2H, s	80.19	-	C2, C6, C7, C15, C21
6	4.03, 2H, s	47.38	-	C2, C5, C7, C15, C16, C17, C18, C21
7	2.68, 1H, m	58.47	H8, H8'	C8, C8'
8	1.25, 2H, m	31.59	H7, H8, H9, H9', H10	C7
8'	1.98,2H, d, br	31.59	H7, H8', H9, H9'	C7
9	1.58, 2H, m	26.30	H8, H8', H9', H10	C8, C8'
9'	1.74, 2H, m	25.94	H8, H8', H9, H10	-
10	1.12, 2H, m	25.50	H8, H9, H9'	C9'
11	2.62, 1H, tt (11.81, 3.30)	57.99	H12, H12'	C12, C12'
12	1.40, 2H, qd (12.09, 2.75)	27.64	H11, H12', H13, H14	C11
12'	1.92, 2H, d, br	27.64	H11, H12, H13, H13', H14	C11, C13
13	1.60, 2H, m	26.30	H12', H13', H14	C12, C12'
13'	1.76, 2H, m	26.01	H12, H12', H13, H14	C11, C13
14	1.16, 2H, m	25.50	H12, H12', H13, H13'	C13'
15	-	151.58	-	-
16	-	121.91	-	-
17	6.66, 1H, d (1.51)	126.76	H19	C2, C6, C15, C16, C19
18	-	128.71	-	-
19	6.83, 1H, d (1.51)	130.18	H17	C2, C6, C15, C17
20	-	124.91	-	-
21	-	155.94	-	-
22	-	122.44	-	-
23	6.74, 1H, d (1.94)	129.04	H26	C1, C3, C21, C26
24	-	127.48	-	-
25	6.64, 1H, d (8.24)	115.63	H26	C1, C21, C24
26	6.89, 1H, dd (8.24 and 1.94)	128.52	H23, H25	C1, C21, C23

Table 1. (Apirat et al.)

Selected Geometry Parameters

(A) Intramolecular Bond Length[a]

O(1) – C(10)	1.369(2)	O(3) – H(3)	0.93(2)
C(5) – C(10)	1.394(2)	O(1) – H(1)	0.94(2)
C(5) – C(6)	1.510(5)	N(2)···H(1)	1.798(6)
N(2) – C(6)	1.477(2)	O(3)···H(1)	2.405(9)
N(2) – C(9)	1.482(2)	N(2)···O(1)	2.624(1)
C(7) – C(9)	1.506(1)	O(3)···H(1)	3.013(1)
C(7) – C(8)	1.394(2)	O(1)···O(3)	3.040(1)
O(3) – C(8)	1.366(2)		

(B.1) Intramolecular Bond Angles

N(2)··· H(1) - O(1)	144.6(1)
H(1) - O(1) - C(10)	111.6(1)
O(1) - C(10) - C(5)	120.9(1)
C(10) - C(5) - C(6)	120.1(1)
C(5) – C(6) - N(2)	113.3(4)
C(6) – N(2) – C(9)	110.5(1)
N(2) – C(9) – C(7)	111.7(1)
C(9) – C(7) - C(8)	120.2(2)
C(7) – C(8) – O(3)	117.3(1)
C(8) – O(3) – H(3)	112.9(1)
C(8) - O(3)··· H(1)	90.9(1)
O(3)··· H(1)··· N(2)	90.4(1)
H(1)··· N(2) - C(6)	93.7(1)
H(1)··· N(2) - C(9)	115.7(1)
O(3)··· H(1) - O(1)	124.5(1)

(B.2) Intermolecular Non-Bond Angles

O(1)··· H(3) – O'(3)	176.3(1)

(C) Intramolecular Torsional Angles

H(1) – O(1) - C(10) – C(5)	12.2(1)
O(1) – C(10) - C(5) – C(6)	5.6(1)
C(10) – C(5) - C(6) - N(2)	-38.5(2)
C(5) – C(6) - N(2) – C(9)	158.1(1)
C(6) – N(2) - C(9) – C(7)	-73.3(3)
N(2) – C(9) - C(7) – C(8)	-67.1(1)
C(9) – C(7) - C(8) – O(3)	-1.2(1)
C(7) – C(8) - O(3) - H(3)	174.6(4)

(D) Intermolecular Interatomic Bond Length

O(1)··· H'(3)	1.773(3)	O(1)··· O'(1)	4.210(4)
O(1)··· O'(3)	2.702(1)	N(2)··· N'(2)	7.441(1)

[a] The atomic numbering is referred to in Table 3.

Table 2. (Apirat et al.)

	X	Y	Z	U_{eq} (Å^2)[a]
O1	0.54290(3)	0.49860(7)	0.61750(4)	0.0653(4)
N2	0.57080(3)	0.21790(7)	0.65030(4)	0.0415(3)
O3	0.49630(3)	0.28420(8)	0.48650(4)	0.0627(4)
C4	0.59230(4)	0.4425(1)	0.81620(5)	0.0492(5)
C5	0.57300(4)	0.40840(9)	0.74190(4)	0.0413(4)
C6	0.55680(5)	0.25140(9)	0.71330(5)	0.0470(5)
C7	0.46650(4)	0.13210(9)	0.56060(5)	0.0461(5)
C8	0.44990(5)	0.2309(1)	0.50120(5)	0.0505(5)
C9	0.53340(4)	0.09020(9)	0.60670(5)	0.0483(5)
C10	0.56270(4)	0.52510(9)	0.69200(5)	0.0487(5)
C11	0.42000(5)	0.0734(1)	0.57560(6)	0.0557(5)
C12	0.60040(4)	0.5868(1)	0.84280(5)	0.0564(5)
C13	0.57160(5)	0.6705(1)	0.71740(6)	0.0636(6)
C14	0.38830(5)	0.2701(1)	0.45890(6)	0.0630(6)
C15	0.63820(4)	0.2055(1)	0.67330(5)	0.0475(5)
C16	0.35790(5)	0.1111(1)	0.53430(6)	0.0669(6)
C18	0.58950(5)	0.6995(1)	0.79160(6)	0.0651(6)
C19	0.61930(9)	0.6187(2)	0.92390(7)	0.090(1)
C23	0.72100(7)	0.2128(2)	0.62890(9)	0.095(1)
C25	0.34330(6)	0.2104(1)	0.47600(7)	0.0691(7)
C26	0.65200(6)	0.2164(2)	0.60630(6)	0.0756(8)
C27	0.74000(6)	0.0801(2)	0.7445(1)	0.101(1)
C28	0.75250(8)	0.0812(2)	0.6773(1)	0.105(1)
H4	0.5997(3)	0.3613(9)	0.8514(4)	0.041(2)
H6A	0.5759(4)	0.179(1)	0.7546(5)	0.055(3)
H6B	0.5109(5)	0.2403(9)	0.6948(5)	0.055(3)
H9A	0.5349(4)	0.0088(9)	0.6419(5)	0.047(2)
H9B	0.5509(4)	0.057(1)	0.5724(5)	0.049(2)
H11	0.4306(5)	0.004(1)	0.6167(6)	0.063(3)
H13	0.5628(5)	0.750(1)	0.6801(6)	0.067(3)
H14	0.3783(5)	0.345(1)	0.4170(6)	0.068(3)
H15	0.6557(4)	0.2960(9)	0.7040(5)	0.049(2)
H18	0.5951(5)	0.799(1)	0.8100(6)	0.072(3)
H19A	0.3136(9)	-0.055(3)	0.571(1)	0.20(1)
H19B	0.273(1)	0.034(2)	0.510(1)	0.150(7)
H19C	0.3002(9)	0.112(2)	0.584(1)	0.191(9)
H20A	0.6238(7)	0.535(2)	0.9558(9)	0.136(6)
H20B	0.5988(8)	0.698(2)	0.9286(9)	0.136(7)
H20C	0.6542(9)	0.671(2)	0.9442(9)	0.149(7)
H23A	0.6533(6)	-0.018(1)	0.6865(8)	0.110(5)
H23B	0.6606(6)	0.065(1)	0.7627(7)	0.094(4)
H24A	0.7414(6)	0.305(1)	0.6542(7)	0.106(5)
H24B	0.7288(7)	0.213(1)	0.5845(8)	0.115(5)
H25	0.3019(6)	0.239(1)	0.4463(6)	0.074(3)
H26A	0.6300(6)	0.313(1)	0.5781(7)	0.094(4)
H26B	0.6316(6)	0.132(1)	0.5744(7)	0.099(4)
H27A	0.7609(7)	-0.001(2)	0.7775(9)	0.132(5)
H27B	0.7562(7)	0.179(2)	0.7752(9)	0.138(6)
H28A	0.7976(8)	0.090(2)	0.6967(8)	0.134(6)
H28B	0.7344(7)	-0.017(2)	0.6446(8)	0.126(5)
H3	0.4827(6)	0.356(2)	0.4492(7)	0.108(5)
H1	0.5460(6)	0.397(2)	0.6080(7)	0.115(5)

[a] $T = exp[2\pi^2 U]$; $U = U_{iso} = U_{eq}$; $U_{eq} = \frac{1}{3}\sum_{i=1}^{3}\sum_{j=1}^{3} U_{ij} a_i a_j a_i a_j$

The numbering of atom is shown below.

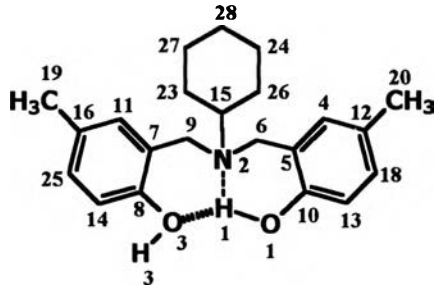

Table 3. (Apirat et al.)

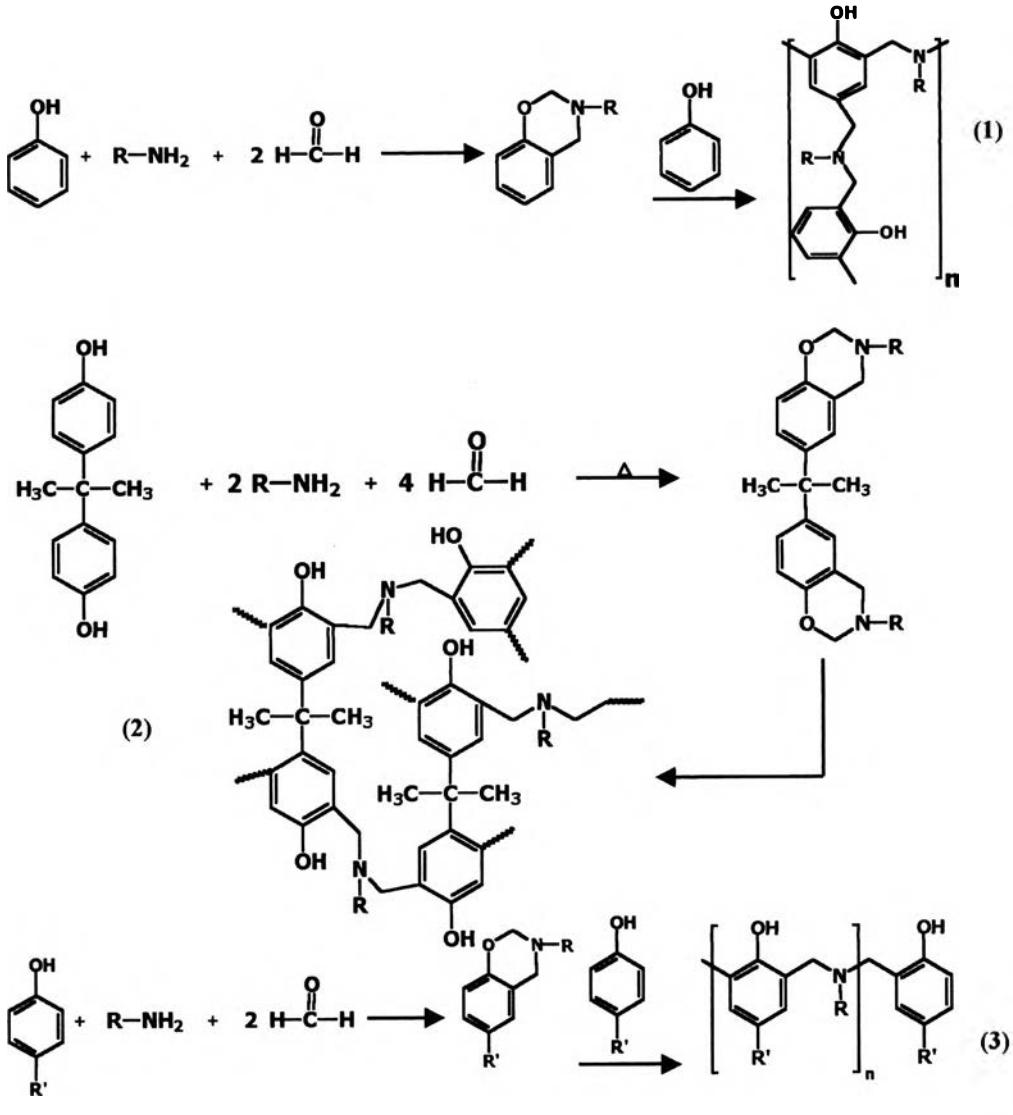

Scheme I. (Apirat et al.)

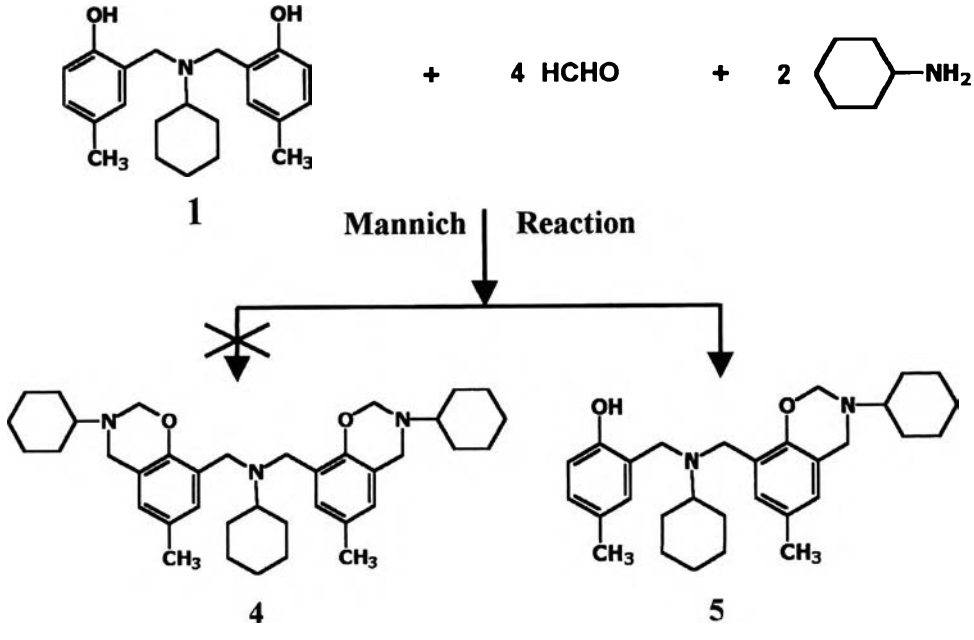

Scheme II. (Apirat et al.)

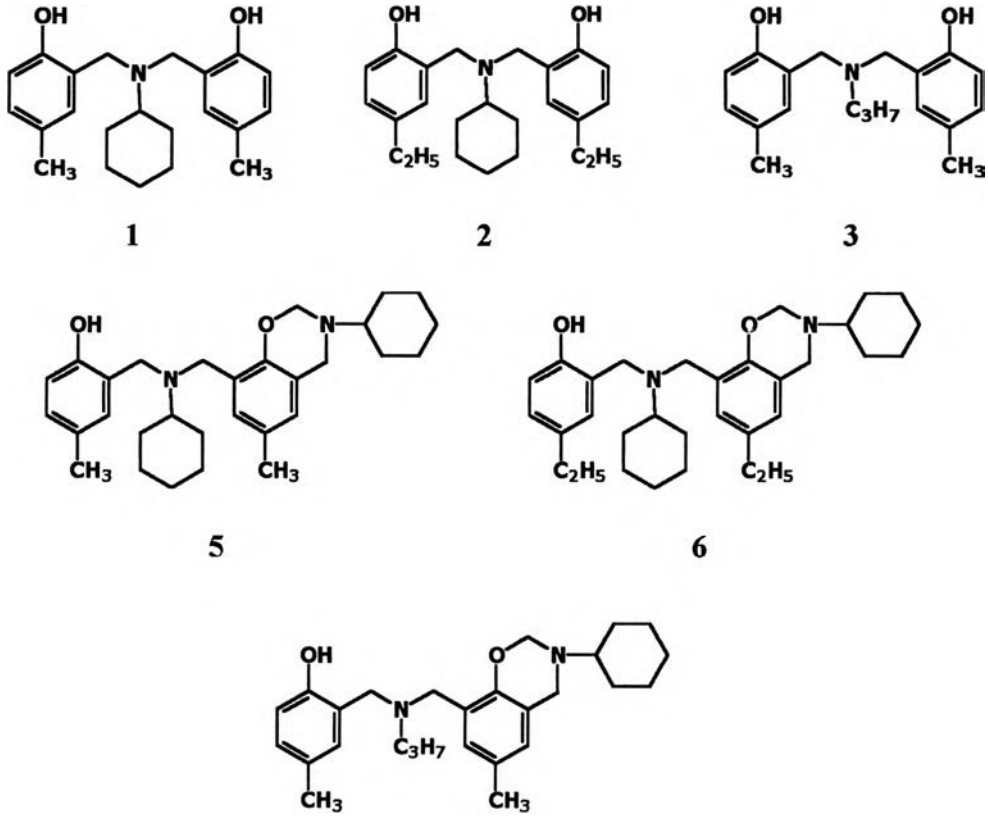

Scheme III. (Apirat et al.)

Supplementary Materials: Figure Captions

Figure I. FT-IR spectra of (a) dimer **1** and (b) mono-oxazine benzoxazine dimer **5**.

Figure II. ^{1}H-NMR spectrum of mono-oxazine benzoxazine dimer **5**.

Figure III. ^{13}C-NMR spectrum of mono-oxazine benzoxazine dimer **5**.

Figure IV. FT-IR spectra of (a) mono-oxazine benzoxazine dimer **5**, (b) mono-oxazine benzoxazine dimer **6**, (c) mono-oxazine benzoxazine dimer **7**.

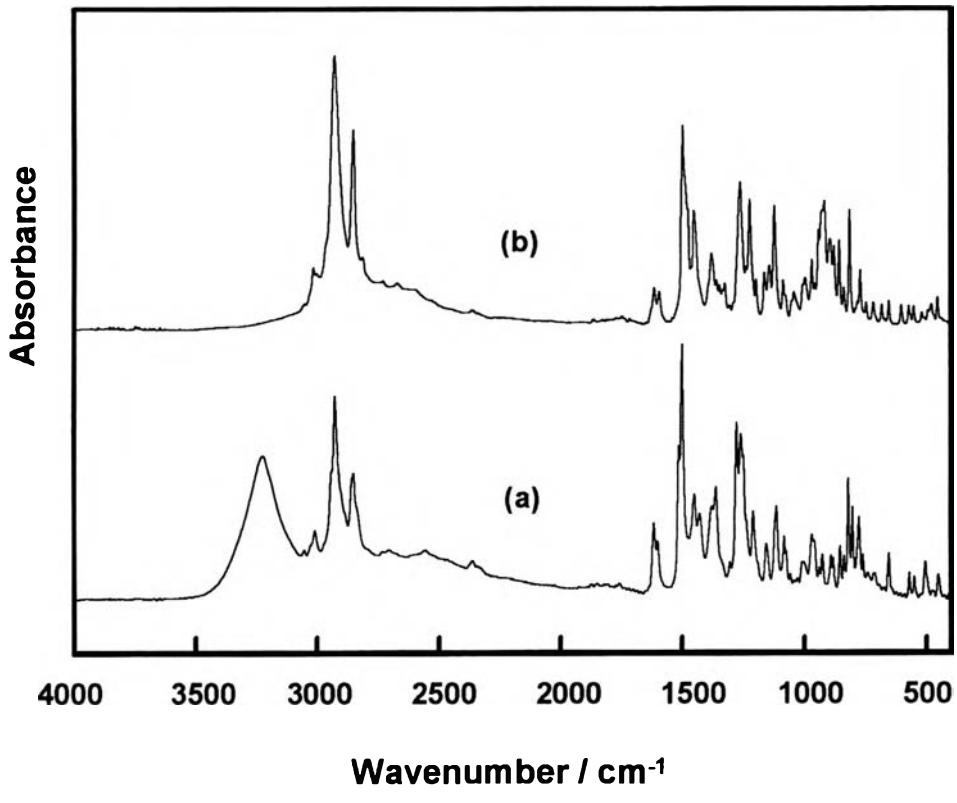

Figure I. (Apirat et al.)

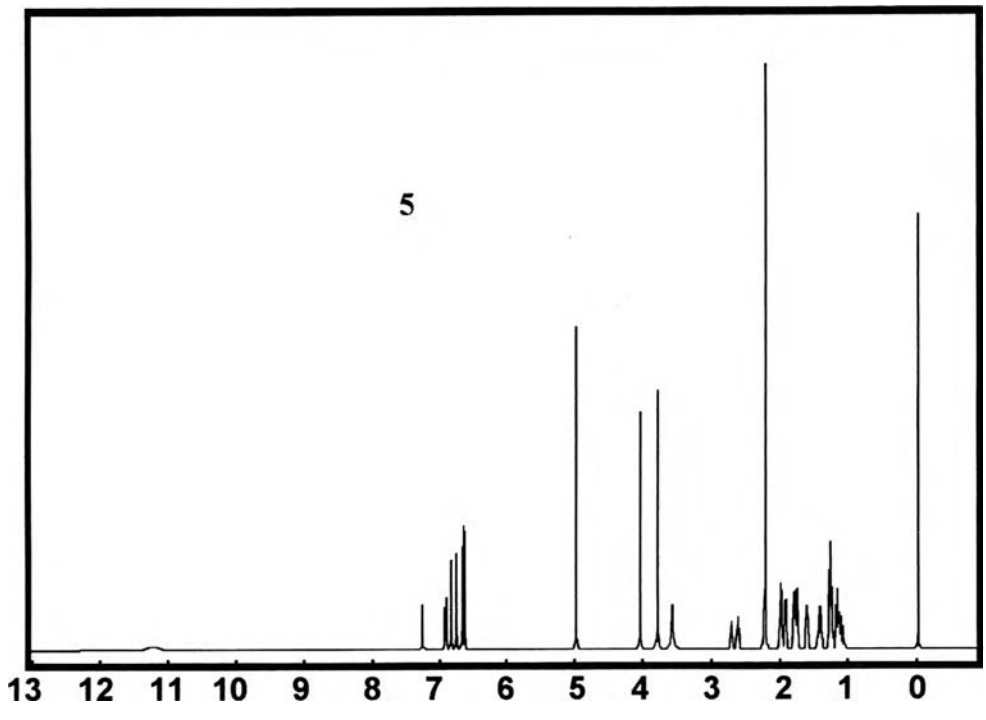

Figure II. (Apirat et al.)

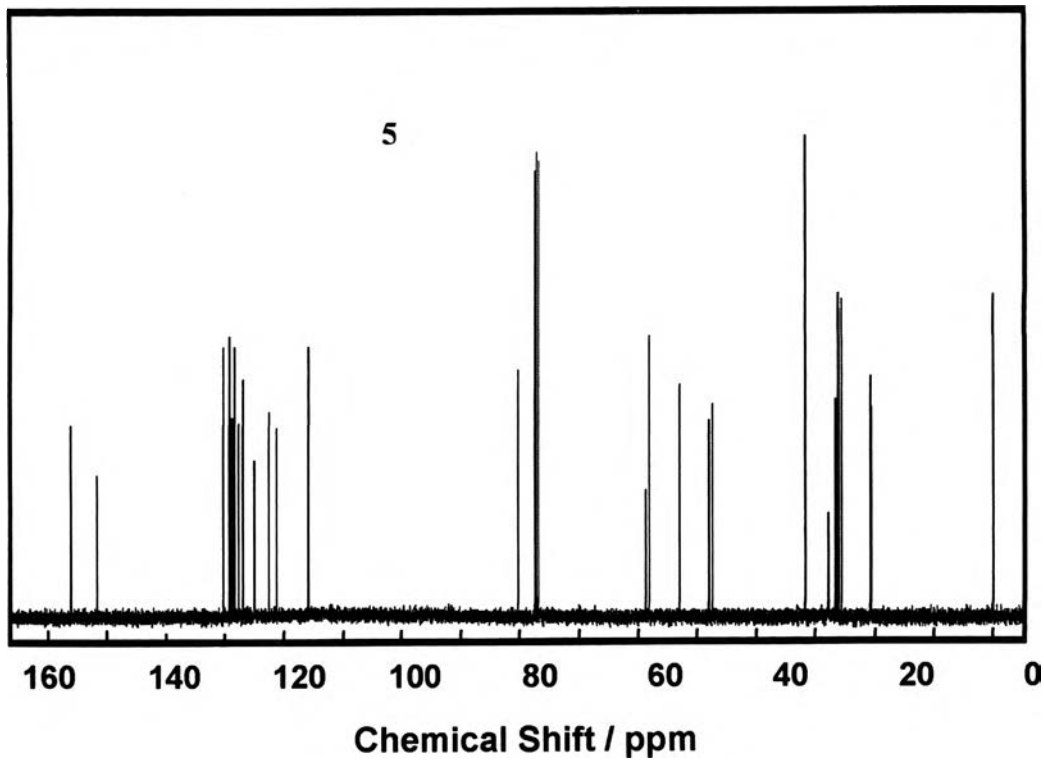

Figure III. (Apirat et al.)

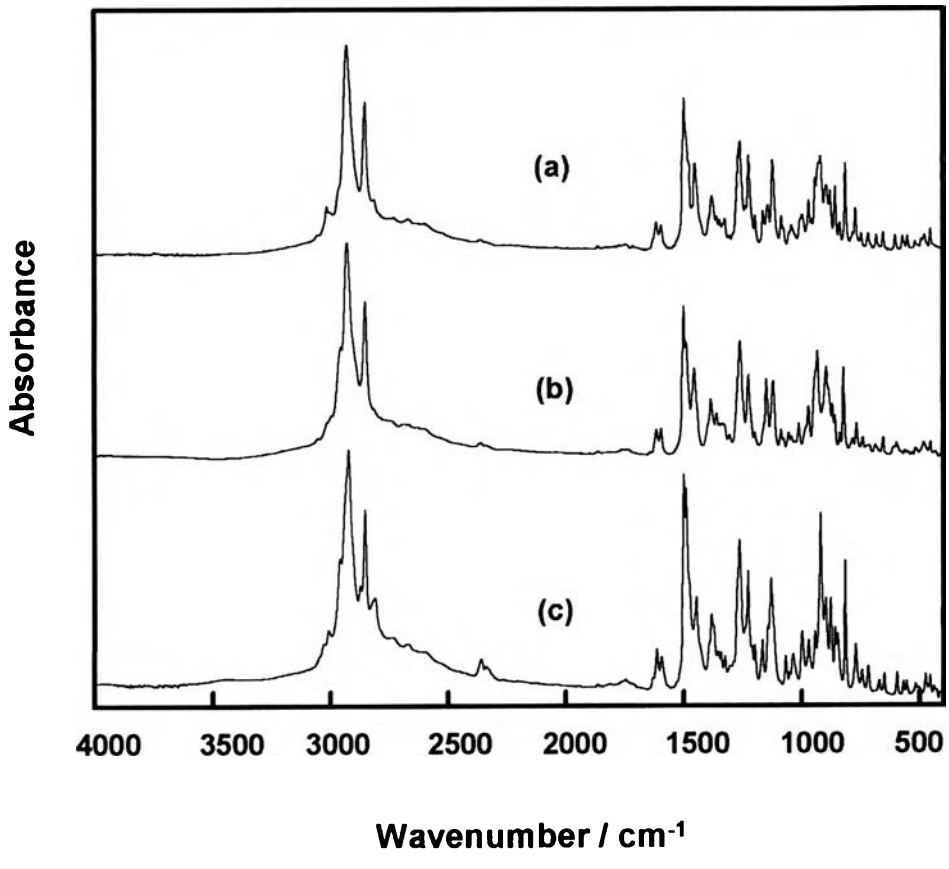

Figure IV. (Apirat et al.)